

## การจำลองแบบพฤติกรรมอัตราความเครียดสูงของโลหะผสมอลูมิเนียมอนุกรม 7108

### Modelling of High Strain Rate Behaviour of a Series 7108 Aluminium Alloy

กุนทีณี มณีรัตน์<sup>1</sup> และ อลอยส์ อีวานโควิช

ภาควิชาวิศวกรรมเครื่องกล อิมพีเรียลคอลเลจ ลอนดอน ประเทศอังกฤษ

<sup>1</sup> ปัจจุบันที่ ภาควิชาวิศวกรรมเครื่องกล คณะวิศวกรรมศาสตร์ จุฬาลงกรณ์มหาวิทยาลัย กทม 10330

Kuntinee Maneeratana<sup>1</sup> and Alojz Ivankovic

Department of Mechanical Engineering, Imperial College, London SW7 2BX, England

E-mail: a.ivankovic@ic.ac.uk

<sup>1</sup> Current Address: Department of Mechanical Engineering, Faculty of Engineering, Chulalongkorn University, Bangkok 10330 Thailand Tel: (02) 218-6644 E-mail: fmekmn@kankrow.eng.chula.ac.th

#### บทคัดย่อ

บทความวิจัยนี้เสนอการจำลองแบบเชิงตัวเลขของการทดลอง split Hopkinson pressure bar (SHPB) ด้วยวิธีคำนวณเชิงตัวเลขแบบปริมาตรจำกัด (FV) เพื่อหาพฤติกรรมของโลหะผสมอลูมิเนียมอนุกรม 7108 ระหว่างอัตราความเค้น 500 ถึง 4000 s<sup>-1</sup> [1]. เนื่องด้วยความสัมพันธ์ความเค้นและความเครียดของวัสดุที่ได้จากการวิเคราะห์ผลการทดลองด้วยวิธีของ Kolsky นั้น ขึ้นอยู่กับความหนาของชิ้นวัสดุตัวอย่าง [2] การหาคุณสมบัติของโลหะผสมจึงกระทำได้โดยการเปรียบเทียบผลจากการจำลองแบบเชิงคณิตศาสตร์กับผลการทดลอง โดยใช้กฎการอนุรักษ์โมเมนตัมเชิงเส้นและพลังงานความร้อนควบคู่กันเป็นสมการหลัก และใช้สมการ Prandtl-Reuss สำหรับการผิดรูปเล็กน้อย อธิบายพฤติกรรมของวัสดุ ตัวแบบทางคณิตศาสตร์แกนสมมาตรที่ได้ ถูก discretise โดยระเบียบวิธีคำนวณเชิงตัวเลขปริมาตรจำกัดแบบ cell-centred ที่สามารถจำลองปริมาตรควบคุมรูปทรงทั่วไป [3, 4] ค่าความสัมพันธ์ระหว่างความเค้นและความเครียดที่ได้จะนำไปใช้หาค่า flow stress และสภาพไวต่ออัตราความเครียดของ flow stress

#### Abstract

This paper describes the finite volume (FV) simulation of a series of split Hopkinson pressure bar (SHPB) experiments on a commercially available

aluminium alloy of series 7108 at strain rates between 500 – 4000 s<sup>-1</sup> [1]. As the stress – strain relationships obtained from the Kolsky analyses of experimental results are dependent on the specimen thickness [2], the experiment is simulated in order to obtain material properties by fitting the numerical results to the experimental measurements. The laws of conservation of linear momentum and thermal energy are employed as governing equations in a coupled manner. The conventional small strain Prandtl-Reuss equation is used to describe material behaviours. The axisymmetric mathematical models are discretised by a cell-centred finite volume technique for arbitrary control volumes [3, 4]. Then, flow stresses are obtained from numerically adjusted stress–strain relationships and the strain rate sensitivity of the flow stress is quantified.

#### 1. Introduction

The compressive SHPB experiment is probably the most popular method of determining properties of materials at high strain rates of up to 10<sup>4</sup> s<sup>-1</sup> as it provides a relatively cheap and simple test with an acceptable level of accuracy [5]. In a test, a specimen, which is a circular disc of uniform thickness, is

sandwiched between two long uniform cylindrical pressure bars (Figure 1). Specimen and bar interfaces are lubricated in order to reduce the friction. The specimen and adjacent sections of the bars are heated to the required temperature by a small furnace.

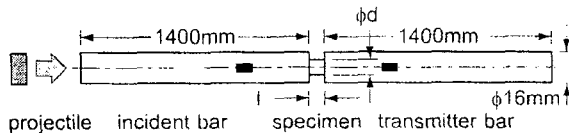


Figure 1 Schematic diagram of the split Hopkinson pressure bar assembly.

A compressive stress pulse is generated in the incident bar by the axial impact of a projectile. The incident wave has approximately rectangular shape with constant amplitude and very short initial rise time. When the stress wave arrives at an interface between the bar and the specimen, parts of the pulse are reflected back and the rest are transmitted through the interface due to the difference in mechanical impedance and cross-sections of the bar and the tested material. The incident, reflected and the transmitted pulse signals are monitored by two strain gauges; one on each pressure bar. The measure strains are converted into stresses and the stress – strain relationship of the tested material may be derived by a suitable integration.

The classical Kolsky analyses [2, 5], which is based on the one-dimensional wave propagation theory, has two main assumptions; the specimen always remains in quasi-static equilibrium and it is subjected to a uniform strain field. In reality, these assumptions can not be fulfilled during the experiment due to various phenomena such as three-dimensional wave reflections, inertia and moving plastic strain fronts in the specimen as well as the frictional constraints at the interfaces, which cause the barrelling of the specimen, etc. [2].

It has been found that the Kolsky analyses of an experiment of a thick specimen give a significantly higher flow stresses than flow stresses obtained from a test of a thinner specimen. This phenomenon has been attributed to the presence of plastic wave propagation, which is a manifestation of large stress gradients. These stress gradients are more severe in a thicker specimen due to the higher impact velocity required to generate a specific strain rate [2]. Moreover, the quasi-equilibrium can be quickly achieved in a thin specimen. These arguments may partly explain why thin specimen tests yield more accurate results. However, tests of thin metal specimens are more susceptible to the frictional effect than those with thick specimens.

There is currently no standard design for the SHPB equipment. The choice of the specimen dimensions is a compromise of several factors [5], though the ratio  $l/d = 0.5\sqrt{3\nu}$ , where  $l$  is the specimen length,  $d$  is the diameter and  $\nu$  is the Poisson ratio of the solid, has been suggested [6].

A series of SHPB tests on specimens of diameter  $d = 10$  mm, fabricated from a precipitation hardened aluminium alloy of series 7108, were conducted at strain rates, ranging from 500 to 3500  $s^{-1}$  and operating temperatures of 24, 280 and 340  $^{\circ}C$  [1]. The dimensions of the test assembly are shown in Figure 1, in which strain gauges are depicted as small black rectangles. Specimens were cut from planar extruded sections and tested with the deformation axis parallel to the extrusion direction. The sizes of the tested specimens can be categorised into two ranges of thickness. Thick specimens have an average  $l/d$  ratio of 0.46, which is similar to the suggested ratio [6]. Meanwhile, specimens with an average ratio of 0.27 are considered to be thin.

The objective of this study is to try reducing the inherent errors of the Kolsky analyses by means of numerical simulations.

As the inertia and plastic wave propagation effects are less severe in thin specimens, the stress – strain curves deduced from the Kolsky analyses from the thin specimen tests should be closer to the actual curves than the ones from the thick specimens. On the other hand, the frictional effects, which are expected to be more pronounced in thin specimens, are much more difficult to quantify. Thus, thick specimen tests are modeled by the finite volume method with the Kolsky stress – strain relations as the initial material properties. Then, the numerical results are compared with the experimental measurements and the input stress – strain curves are iteratively adjusted until the numerical solutions excellently agree the experimental results. The final material properties are expected to be closer to those obtained by the Kolsky analyses from the thin specimen tests, which are known to be more accurate. It is also reasoned that if the geometry independent stress – strain curves, representing the actual material properties, is used in the simulations, the numerical predictions should agree with the experimental results of both thick and thin specimen tests. Then, the flow stresses at 3% plastic strain are obtained and used in the study of the strain rate sensitivity.

## 2. Mathematical Model and Discretisation

The laws of conservation of momentum and thermal energy under small deformation conditions are employed as governing equations. The conventional Prandtl-Reuss relationship between the engineering strain rate and engineering stress rate is used as the constitutive equation of the aluminium alloy. This rate and temperature independent thermo-elastoplastic material also assumes the von Mises yield criterion, associated flow rule and isotropic hardening. In the current study, the average rate and temperature within the specimens are thought not to change appreciably during testing as to affect the material behaviour. This justifies the choice of the constant relationship. The

thermal expansion of the body is assumed to be linear and all the plastic dissipation is converted into heat. Readers interested in more details are directed to [2] and [7].

The axisymmetric mathematical models, which consist of conservation of axial momentum, radial momentum and thermal energy equations, are discretised by a cell-centred finite volume technique for arbitrarily-shaped control volumes [3, 4]. The method assumes fully implicit time discretisation and piece-wise linear distribution in space. Temporal terms are approximated by the mean value theorem while surface and volume integrals are discretised using the mid-point rule. The non-orthogonality in the diffusion term is approximated by an orthogonal correction approach. Thus, the spatial discretisation is second-order accurate while the temporal discretisation is only first-order accurate. The sets of coupled non-linear algebraic equations are segregated, linearised and decoupled. A resulting system of algebraic equations is iteratively solved by an incomplete Cholesky preconditioned conjugate gradient method until a certain level of convergence is obtained. The results of a system are used to update other systems of equations, which are similarly solved in terns. This procedure is repeated until implicit solutions are obtained.

## 3. Numerical Simulations

Only the 700 mm sections of the pressure bars in contact with the specimen are considered in the numerical simulations as they are sufficiently long such that no stress waves reflected back from the free ends will interfere with the recording of stress waves during the calculation at the strain gauge positions. For each test case, the actual dimensions of the specimen are precisely modelled. Uniform meshes are used to avoid spurious wave reflections. Hence, due to the extreme difference between the bar lengths and the specimen thicknesses and the necessity to use fine grid across

the specimens, a typical mesh for each pressure bar consists of 17850 axisymmetric cells. The thick and thin specimens are modelled by 121 and 77 control volumes. In total, the grids for thick and thin specimen test assemblies possess 71646 and 71554 degrees of freedoms, respectively.

The properties of the maraging 300 steel pressure bars are Young's modulus  $E = 182.4 \text{ GPa}$ , Poisson ratio  $\nu = 0.3$ , density  $\rho = 8044 \text{ kg/m}^3$ , linear thermal expansion  $\alpha = 1.1 \times 10^{-5} \text{ K}^{-1}$ , thermal conductivity  $k = 50 \text{ W/mK}$  and specific heat  $c = 450 \text{ J/kgK}$ . The material properties for the alloy are  $\nu = 0.33$ ,  $\rho = 2780 \text{ kg/m}^3$ ,  $\alpha = 2.1 \times 10^{-5} \text{ K}^{-1}$ ,  $k = 140 \text{ W/mK}$  and  $c = 875 \text{ J/kgK}$ . The uniaxial stress – strain relations, which are iteratively obtained as previously described, are smoothed by an exponential best fit  $\sigma = a(1 - e^{-b\epsilon^n})$  where  $\sigma$  and  $\epsilon$  are respectively uniaxial stress and strain, and  $a$ ,  $b$  and  $n$  are constant. The yield stress  $\sigma_y$  is defined by 0.3% offset strain.

All external surfaces are assumed to be stress free. In the experiments, the interfaces between the bars and specimen were sufficiently well lubricated as evidenced by the absence of obvious barrelling of deformed specimens. Therefore, the interfaces are simply considered to be frictionless in the numerical simulations. The absence of friction between the bars and specimen interfaces is incorporated into the code by setting all the contributions from shear stresses to zero at the interfaces and calculating the radial displacement gradients as that of free surfaces accordingly. It is also found that the heat loss from the specimen to the surrounding is negligible due to the extremely short duration of the test such that adiabatic boundary condition may be assumed.

The strain rate, which is applied at the free end of the incident bar, is converted into an equivalent single rectangular compressive stress pulse with amplitude  $\sigma^{\text{pulse}}$ . The duration of the stress pulse was determined from the experimental records to be  $80 \text{ } \mu\text{s}$ . The

computation is performed for  $350 \text{ } \mu\text{s}$  and is divided into 7000 equal time intervals of  $0.05 \text{ } \mu\text{s}$ .

The simulations are conducted on a digital DEC alpha station 500. On average, it takes 8.5 hours for every calculation. The number of iterations needed to adjust the stress – strain relationships depends on the desired accuracy; in most cases five or six iterations are sufficient. In some cases, however, twice that number of iterations may be necessary.

#### 4. Comparisons and Evaluations of Results

Figure 2 compares typical experimental measurements of axial stresses at the strain gauge positions with results from simulations of a thick specimen with the ratio  $l/d = 0.45$ . The corresponding Kolsky and numerically fitted stress – strain curves are shown in Figure 3.

It is clear that the solutions of the numerical simulations using Kolsky stress – strain relations do not agree very well with the experimental measurements of the thick specimen test. With the iterative adjustments, the numerically fitted stress – strain relation can be obtained such that the numerical predictions are in excellent agreements with the experimental results.

The numerical stress – strain relations obtained from the thick specimen tests are, then, used to simulate thin specimen tests at similar strain rates and operating temperatures. If the thick specimen stress – strain curves are geometry independent material properties, the simulation of the thin specimen tests should produce satisfactory comparisons of numerical predictions with the experimental results.

Figure 4 compares experimental measurements of a thin specimen ( $l/d = 0.28$ ) test with numerical results from finite volume simulations using the Kolsky stress – strain curve and the predicted relation from a thick specimen ( $l/d = 0.45$ ) test at a similar strain rates. (These stress – strain relationships can be found in Figure 3.) It is found that the modeling which uses the

predicted material properties agrees with the experimental measurements better than the simulation using the stress – strain relation obtained by the Kolsky analyses of the experimental results.

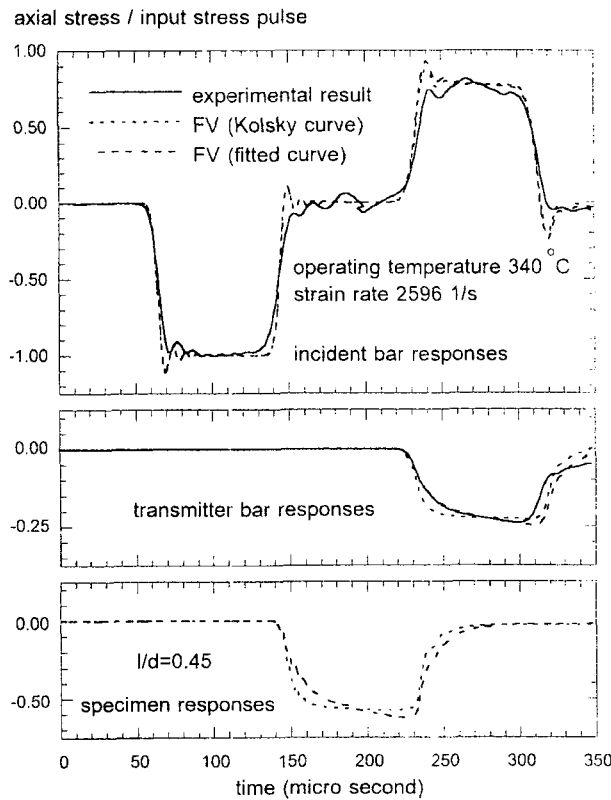


Figure 2 Comparisons of experimental results of a thick specimen SHPB test with the numerical results using the Kolsky and numerically fitted stress – strain curve.

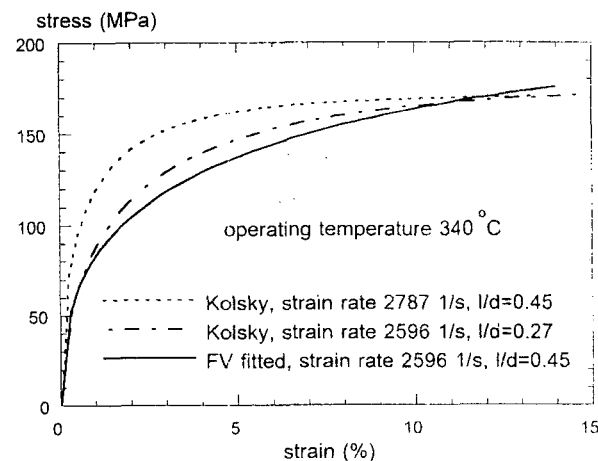


Figure 3 Comparison of stress – strain relations obtained from the Kolsky analyses and numerical fitting.

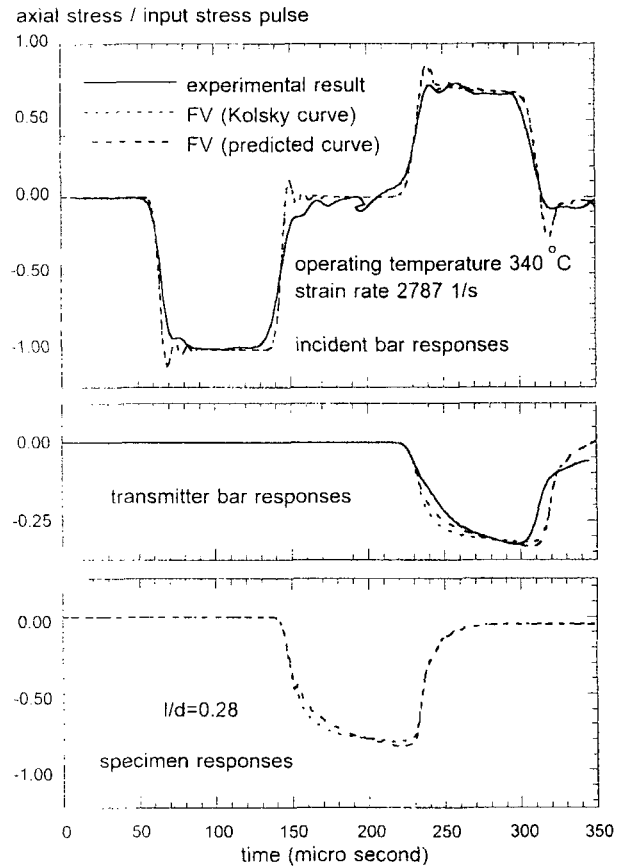


Figure 4 Comparisons of experimental results of a thin specimen SHPB test with the numerical results using the Kolsky and numerically fitted stress – strain curve.

By simulating several thick specimen tests, the numerically fitted stress – strain relations at different strain rates and operating temperatures are compiled. Then, the flow stresses at 3% plastic strain, which are simply specified [1], are obtained from the curves as shown in Figure 5.

It is well known that the flow stresses have a general tendency to increase with an increased rate of loading and a decreased operating temperatures. In this section, the strain rate sensitivities of the alloy are quantitatively analysed. The effect of strain rate sensitivity is most frequently described by an empirical power law  $\sigma_{\text{fl}} = k' \dot{\epsilon}^m$ , where  $\sigma_{\text{fl}}$  is the flow stress,  $k'$  is a coefficient,  $\dot{\epsilon}$  is the strain rate and the exponent  $m$  is the strain rate sensitivity index which may depend on strain, strain rate and temperature [8]. According to the

review of the microscopic rate controlling mechanism [1], the strain rate sensitivities are expected to be low as the alloy is precipitation hardenable and tested in the peak tempered and overaged condition.

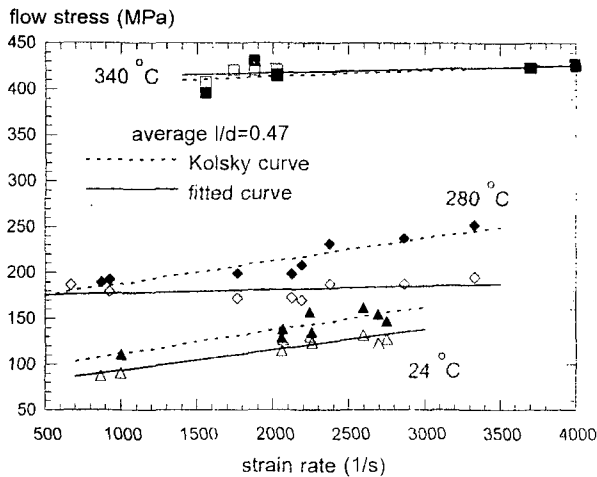


Figure 5 The strain rate and flow stress at 3% plastic strain obtained from the Kolsky analyses and numerical fitting.

In a general procedure, the sensitivity index  $m$  is obtained as the slope of the linear relationship  $\ln(\sigma_p) = m \ln(\dot{\epsilon}) + \ln(k')$ . Figure 6 shows the natural log — natural log relationship between the strain rate and flow stress obtained from the Kolsky curves of thick and thin specimens as well as the thick specimen numerically fitted stress — strain relations.

In addition to the SHPB results, the flow stresses obtained from servo-hydraulic tests, in which constant strain rates were achieved by controlling crosshead velocity during the tests, at low and medium strain rates between  $0.1$  and  $100 \text{ s}^{-1}$  are used [1].

The values of sensitivity index  $m$ , obtained from the SHPB and servo-hydraulic data as well as servo-hydraulic values only, are summarised in Table 1. As expected, this alloy has a relatively low strain rate sensitivity which slightly increases with temperature. Figure 6 also show that the sharp increase of strain rate sensitivity, predicted by the Kolsky analyses is very likely to be artificial and not a real material response.

Numerical results, on the other hand, show much reduced strain rate sensitivities

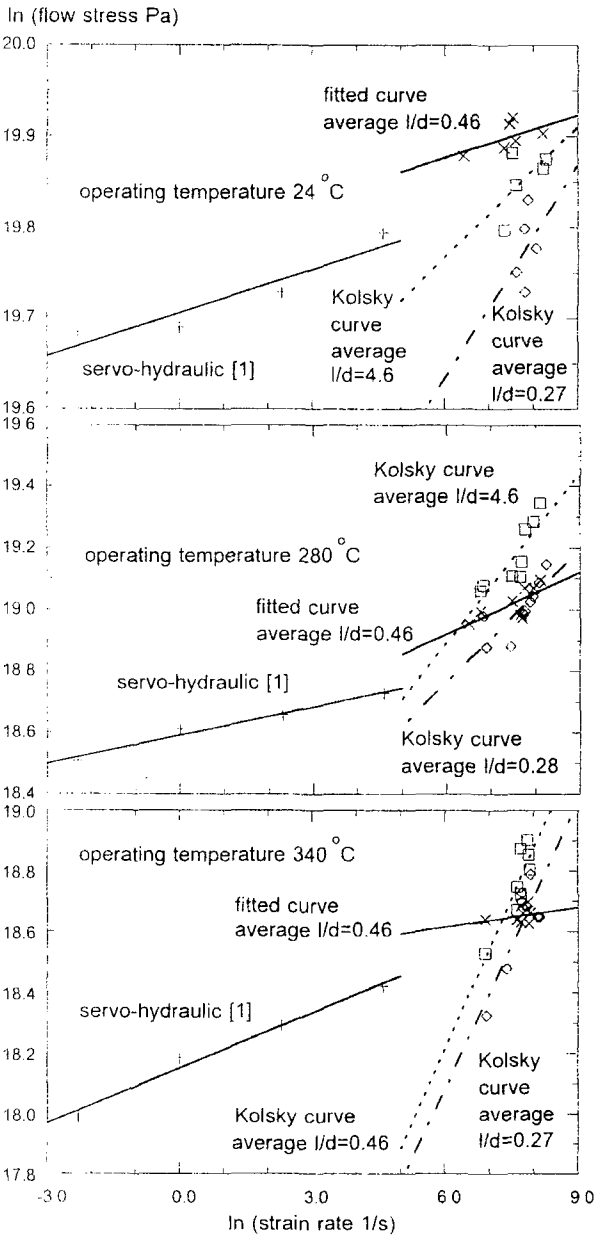


Figure 6 Natural log — natural log relationship between the strain rate and flow stress at 3% plastic strain obtained from the Kolsky analyses and numerical fitting.

Table 1 Compilation of the sensitivity index  $m$  obtained from the low strain rate data [1] together with Kolsky or numerically fitted curves.

temp (°C)	only servo-hydraulic	Kolsky curve		fitted curve
		$l/d=0.46$	$l/d=0.27$	
24	0.0160	0.0200	0.0109	0.0232
280	0.0309	0.0466	0.0766	0.0587
340	0.0608	0.0891	0.0631	0.0655

## 5. Conclusions

Series of SHPB tests on a series 7108 aluminium alloys at different strain rates and operating temperatures were simulated using the finite volume technique with a transient thermo-elastoplastic material model. The stress – strain relations at specific strain rates and temperatures were obtained by iteratively adjusting the material properties until numerical results excellently agreed with experimental measurements. The flow stresses at 3% plastic strain were obtained from the numerically data. Then, the strain rate sensitivity of the flow stresses was calculated. When results from the Kolsky and numerical analyses were compared, it was found that the sharp increase of flow stress which is predicted by Kolsky analyses is likely to be artificial and not a real material response.

Even though it is presumptuous to state that the numerically obtained stress – strain relations are the true material properties, it can be confidently concluded that numerical simulations can be used to reduce inherent errors from the Kolsky-deduced analyses. Future works should concentrate on developing a rate and temperature dependent large strain material model as well as studying the effects of friction at the interfaces between the bars and the specimens.

## References

- [1] L.J. Djapic-Oosterkamp, A. Ivankovic, and G. Venizelos, "High strain rate properties of selected Aluminium alloys", *Materials Science and Engineering*, A278, 2000, pp. 225-235.
- [2] N.N. Diah, A. Ivankovic, P.S. Leever and J.G. Williams, "Stress wave propagation effects in Split Hopkinson Pressure Bar Test", *Proceedings of the Royal Society of London Series A – Mathematical and Physical Sciences*, vol. 449, no. 1936, 1995, pp. 187-204.
- [3] I. Demirdzic and S. Muzaferija, "Numerical method for coupled fluid flow, heat transfer and stress analysis using unstructured moving mesh with cells of arbitrary topology" *Computer Methods in Applied Mechanics and Engineering*, vol. 125, 1995, pp. 235-255.
- [4] H.G. Weller, G. Tabor, H. Jasak and C. Fureby, "A tensorial approach to computational continuum mechanics using object oriented techniques", *Computers in Physics*, vol. 12, no. 6, 1998, pp. 620-631.
- [5] M.M. Al-Mousawi, S.R. Reid and W.F. Deans, "The use of the split Hopkinson pressure bar techniques in high strain rate materials testing" *Proceedings of the Institution of Mechanical Engineers Part C – Journal of Mechanical Sciences*, vol. 211, no. 4, 1997, pp.273-292.
- [6] E.D.H. Davies and S.C. Hunter, "The dynamic compression testing of solids of the method of split Hopkinson pressure bar, *Journal of the Mechanics and Physics of Solids*, vol. 11, pp. 155-181.
- [7] I. Demirdzic and D. Martinovic, "Finite volume method for thermo-elasto-plastic stress analysis", *Computer Methods in Applied Mechanics and Engineering*, vol. 109, 1993, pp. 331-349.
- [8] R.H. Wagoner and J. Chenot, "Fundamentals of Metal Forming", John Wiley & Sons, New York.